Formation of highly oxygenated organic molecules from chlorine atom initiated oxidation of alpha-pinene

Yonghong Wang[1], Matthieu Riva[1,2], Hongbin Xie[3,1], Liine Heikkinen[1], Simon Schallhart[1], Qiaozhi Zha[1], Chao Yan[1], Xu-Cheng He[1], Otso Peräkylä[1] and Mikael Ehn[1]

[1]Institute for Atmospheric and Earth System Research / Physics, Faculty of Science, P. O. Box 64, 00014 University of Helsinki, Helsinki, Finland

[2]Univ Lyon, Université Claude Bernard Lyon 1, CNRS, IRCELYON, F-69626, Villeurbanne, France

[3]Key Laboratory of Industrial Ecology and Environmental Engineering (MOE), School of Environmental Science and Technology, Dalian University of Technology, Dalian 116024, China

Revised to: Atmospheric Chemistry and Physics

Corresponding to: Yonghong Wang and Hongbin Xie

yonghong.wang@helsinki.fi; hbxie@dlut.edu.cn

Abstract

Highly oxygenated organic molecules (HOMs) from atmospheric oxidation of alpha-pinene can irreversibly condense to particles and contribute to secondary organic aerosol (SOA) formation. Recently, the formation of nitryl chloride ($ClNO_2$) from heterogeneous reactions, followed by its subsequent photolysis is suggested to be an important source of chlorine atoms in many parts of the atmosphere. However, the oxidation of monoterpenes such as alpha-pinene by chlorine atoms has received very little attention, and the ability of this reaction to form HOM is completely unstudied. Here, chamber experiments were conducted with alpha-pinene and chlorine under low and high nitrogen oxide (NO_x, $NO_x = NO + NO_2$) conditions. A nitrate-based CI-APi-TOF (Chemical Ionization-Atmospheric Pressure Interface-Time of Flight) was used to measure HOM products. Clear distributions of monomers with 9-10 carbon atoms and dimers with 18-20 carbon atoms were observed under low NO_x conditions. With increased concentration of NO_x within the chamber, the formation of dimers was suppressed due to the reactions of peroxy radicals with NO. We estimated the HOM yields from chlorine-initiated oxidation of alpha-pinene under low-NO_x conditions to be around 1.8 %, though with a substantial uncertainty range (0.8-4 %) due to lack of suitable calibration methods. Corresponding yields at high NO_x could not be determined because of concurrent ozonolysis reactions. Our study demonstrates that chlorine atoms also initiated oxidation of alpha-pinene and yields low volatility organic compounds.

1. Introduction

Highly oxygenated organic molecules (HOMs) have been identified as key species in the formation of new atmospheric aerosol particles and secondary organic aerosol (SOA) (Ehn et al., 2014, 2017; Kulmala et al., 2013; Bianchi et al., 2019). Recently, the formation of HOMs in the gas phase was described as an autoxidation process of peroxy radicals (RO_2) via multiple intramolecular H atom shifts (Crounse et al., 2013; Jokinen et al., 2014b; Mentel et al., 2015; Rissanen et al., 2014). Oxygen-containing moieties such as carbonyl, carboxylic acid and hydroxyl groups can weaken nearby C-H bonds, making H-abstraction and autoxidation competitive with bimolecular RO_2 reactions, e.g. with NO (Crounse et al., 2013; Praske et al., 2018). Until now, all studies on the formation of HOMs have focused on reactions initiated by oxygen-containing oxidants (O_3 and OH)(Berndt et al., 2016; Ehn et al., 2014; Jokinen et al., 2015).

Increasing evidence indicates that the chlorine atom (Cl) may also play an important role in transforming atmospheric organics (Tham et al., 2016; Thornton et al., 2010). Chlorine atoms have the greatest reactivity toward volatile organic compounds (VOC), with rate constants that are, with some exceptions, an order of magnitude higher than those of hydroxyl radicals (OH) (Riva et al., 2015). Historically, chlorine atoms were thought to be formed primarily from heterogeneous reaction cycles involving sea salt, and their concentrations estimated to be around 1-10% of that of OH (Thornton et al., 2010). Therefore, the role of chlorine atoms in atmospheric oxidation processes has traditionally been thought to be limited to the marine boundary layer only. In recent years, $ClNO_2$, as a significant chlorine atom source, was found in continental regions of America, Canada and Germany, and high concentrations of $ClNO_2$ were also detected in the urban atmosphere in China (Reyes-Villegas et al., 2018; Tham et al., 2016; Thornton et al., 2010; Wang et al., 2017). The new findings have expanded the potential importance of chlorine atoms from coastal areas to continental urban areas. A recent study also reported that chlorine atoms can be more important than OH radicals

for the oxidation of alkanes in the North China Plain (Liu et al., 2017). Therefore, it is desirable to probe the role of chlorine radicals in the degradation of VOCs and related SOA formation.

Emission of biogenic volatile organic compounds (BVOC) to the atmosphere dominates total hydrocarbon emissions on a global scale, with methane, isoprene and terpenes having the highest source strengths (Guenther et al., 2012). Alpha-pinene is the most abundant monoterpene in the atmosphere and its oxidation products from ozonolysis and photooxidation contribute to a substantial fraction of SOA mass (Riccobono et al., 2014; Zhang et al., 2018). Many of the regions listed earlier, where $ClNO_2$ was identified as a chlorine atom source, may also have substantial monoterpene emissions, making Cl a relevant oxidant also for BVOC. Chlorine atom initiated reactions of alpha-pinene have also been shown to contribute to the formation of SOA, which implies that low volatile compounds are efficiently produced also in this process (Cai and Griffin, 2006; Ofner et al., 2013).

Similar to the reaction with OH radicals, the reaction of VOCs with chlorine atoms may proceed either via addition of Cl to unsaturated bonds or via H-abstraction. Wang et al., (2017) found that the Cl addition to isoprene can lead to the formation of low volatility organic compounds. In principle, Cl-initiated reactions could form HOMs in a similar manner as OH-initiated reactions (Berndt et al., 2016a), as the initial addition or abstraction step is comparable for both oxidants. In view of the increased understanding of the importance of chlorine atoms in atmospheric chemistry, it is desirable to investigate the formation of HOMs from reactions of common atmospheric VOC with Cl.

Here, laboratory chamber experiments were performed to investigate the ability of chlorine atom to form HOMs from the oxidation of alpha-pinene. HOMs were characterized using a nitrate-based chemical ionization mass spectrometer, under both

low and high NO_x conditions. The yields of these HOMs were determined under the low NO_x conditions, and the atmospheric implications of this study are discussed.

2. Experiment and method

2.1 Experimental setup

The experiments were conducted in the "COALA" chamber at the University of Helsinki (Peräkylä et al., 2019; Riva et al., 2019). It is a 2 m^3 Teflon chamber, run as a continuously stirred tank reactor, used with a flow of 45 liter per minutes (LPM), resulting in an average residence time of about 45 minutes. The chamber is surrounded by housing to provide dark conditions. No water vapor was added to the chamber, resulting in an RH<1 %, and the temperature was the same as the temperature of the room, around 25°C. The HOM formation targeted in this work is not expected to change markedly as a function of RH, as also indicated in a previous study on both ozone and OH initiated oxidation of monoterpenes (Li et al., 2019). Although SOA mass yields were not studied in this work, these may be affected by RH (Jonsson et al., 2006, 2008). A general schematic of the chamber facility is shown in Figure 1. Our experiment was aimed to probe chlorine atom initiated formation of HOMs under low/high NO_x conditions. We use 400 nm LED lights to photolyze chlorine and NO_2 and produce chlorine atoms and NO as following:

$$NO_2 \rightarrow NO + O$$

$$Cl_2 \rightarrow Cl + Cl$$

The concentration of Cl atoms was varied by changing the amount of 400 nm light. In practice this was done by turning on different amounts of the available lights, with the maximum corresponding to seven. We will refer below to the number of lights that were turned on, although each "light" corresponds to a group of LED strips.

2.2 Instrumentation and data analysis

A nitrate ion (NO_3^-) based chemical ionization atmospheric pressure interface long time-of-flight (CI-APi-L-TOF) mass spectrometer was used for measuring HOMs. The instrument has been shown to be sensitive towards this group of compounds, detecting them as adducts with the nitrate ion. Due to a lack of suitable calibration methods, the CI-APi-TOF was not calibrated for HOMs during this study. In order to estimate rough HOM concentrations ([HOM]), we directly use the calibration coefficient C = 1.6 e10 molec cm^{-3} utilized by Ehn et al. (2014), to convert the measured HOM ion signals according to the equation below (Jokinen et al., 2014).

$$[HOM] = C * \frac{HOM \cdot NO_3^-}{NO_3^- + HNO_3 \cdot NO_3^-}$$

This value of C is very close to values utilized in several other studies using a CI-APi-TOF (Jokinen et al., 2014, 2015; Riva et al., 2019). Ehn et al (2014) obtained their calibration factor from a permeation source using a perfluorinated acid, and also showed through calculations that there were theoretical limitations for having a much larger or a much smaller value for C.

This approach obviously brings large uncertainties to the HOM concentrations, which we estimate to be at least -50 %/+100 % according to previous calibration results (Jokinen et al., 2014, 2015; Riva et al., 2019). More detailed information about the instrument can be found in (Jokinen et al., 2012), noting that compared with the CI-APi-TOF used before, the long time-of-flight mass spectrometer used here has a doubled mass resolving power enabling a more accurate assignment of molecular formulas. Simultaneously, we also used a high-resolution long time-of-flight aerosol mass spectrometer (HR-L-TOF-AMS) to measure bulk aerosol chemical properties (Decarlo et al., 2006). As no seed aerosol particles were added to the chamber, the VOC oxidation products lead to new particle formation and growth to large enough sizes to be measured by the AMS. We also periodically used a filter in front of the AMS inlet to see the influence of the background signal to measured aerosol mass concentration. There were 10 minutes of filter measurements per hour during our experiments. A PTR-TOF-MS (TOF-8000, Ionicon) was used to measure the concentration of alpha-pinene in the chamber. The instrument background was determined every day for 20 mins by

guiding the chamber air through a catalytic converter, which removes the VOCs. Then, the background corrected signals were used to obtain alpha-pinene mixing ratios by using the calibration coefficient determined before the experiments. A description of the used setup employed for the calibration and zero air measurements have been introduced earlier (Schallhart et al., 2018). A custom-built DMPS system was used to measure the particle number size distribution from 10 nm to 400 nm in the chamber. The NO concentration was measured with an ECO-PHYSICS CLD 780 TR instrument with a detection limit of 3 ppt. NO_x (=NO+NO_2) concentrations were determined by using a Thermo-Fisher 42i analyzer. O_3 concentration was measured with a Thermo-Fisher 49i analyzer.

2.3 Estimation of chlorine atom concentrations

During steady state in the chamber, average concentrations of chlorine atom was calculated using the rate coefficients (4.6±1.3) • 10^{-10} cm^3 $molecule^{-1}$ s^{-1} of Cl atoms with alpha-pinene (Finlayson-Pitts et al., 1999), as following:

$$d[AP]/dt = Q\_in - k * [Cl] * [AP] - Q\_out$$

where Q _in is the flow rate of alpha-pinene continuously injected into the chamber, and Q_out is the flow rate that exited the chamber. The term Q_in related concentration was 13.3 ppb, while the term Q_out varied depending on the conditions, and is calculated as [AP]/45 min. During steady state, d[AP]/dt is zero, and then [Cl] concentration is calculated accordingly. As shown in Figure 2, the concentration of HOMs decreased and alpha-pinene increased as the number of lights switched on changed from 7 to 4, 2 and 1. We use the variation of alpha-pinene and HOM concentrations during this run to calculate both chlorine atom concentrations and HOM yields. Each change in alpha-pinene concentration was due to the change in Cl atom concentration, and with knowledge of the reaction rate, the concentration of Cl atoms as a function of the number of lights turned on was determined (Figure 3). The calculated [Cl] concentrations are in the range of (1-5) x 10^5 molecules cm^{-3}, which is within atmospheric relevant concentration ranges (Tham et al., 2016). Raw data from

the CI-API-L-TOF were recorded in 10s resolution in HDF format. We used Toftools for data analysis and detailed protocols of the software have been introduced by Junninen et al. (2010).

2.4 HOMs molar yield

The change of HOM concentration with time can be described as follows, in analogy with Ehn et al. (2014):

$$\frac{d[HOMs]}{dt} = k_1 g[\alpha\text{-}pinene][Cl] - k_{loss}[HOMs] \quad (1)$$

$$g = \frac{k_{loss}[HOMs]}{k_1[\alpha\text{-}pinene][Cl]} \quad (2)$$

Here, k_1 is the reaction rate coefficient of alpha-pinene with chlorine atoms and γ is the molar yield of HOMs, i.e., the fraction of alpha-pinene + Cl reactions that produced HOMs. k_{loss} is the loss rate of HOMs to the chamber walls and particles, though the latter was negligible in this study due to the low aerosol loadings. We used 300 s as a lifetime of HOMs, i.e. k_{loss} = 1/300 s^{-1}, in our previous study in the COALA chamber (Riva et al., 2019).

3. Results and discussion

3.1Formation of HOMs under low NO condition

Figure 4 (a, b, c and d) shows mass spectra measured by the NO_3-CI-APi-TOF during steady state alpha-pinene oxidation with different amounts of lights switched on. The

x-axis represents mass to charge ratio, in units of Thomson (Th). The y-axis represents signals in units of counts per second. As we can see, both monomers (280-400 Th) and dimers (440-580 Th) showed increased signals with increased number of lights, and consequently increased [Cl]. The most abundant peaks are labeled in Figure 4d, with some of the largest signals in the monomer range attributed to $C_9H_{12}O_{7,8}$ and $C_{10}H_{14}O_{8,9,10}$.The formation of both groups could correspond to the oxidation being initiated by H-atom abstraction by Cl, and final termination (from uni- or bimolecular reactions) leading to loss of OH or HO_2. For the C_9 compounds, an additional loss of formaldehyde (CH_2O) during the oxidation process would explain the amount of observed C and H atoms. During the oxidation of $C_{10}H_{16}$, in the absence of NO, the fate of RO_2 radicals depends on the concentrations of HO_2 and RO_2. Autoxidation competes with bimolecular reactions, becoming more likely at lower RO_2 and HO_2 concentrations.

As we show in the Figure 4(d), $C_{10}H_{14}O_{8\text{-}12}$ compounds are large peaks in the monomer range observed with the NO_3-CI-API-TOF. These compounds with 14 hydrogens may come from decomposition of $C_{10}H_{15}O_n$ peroxy radicals via loss of OH or HO_2, or following reactions with other RO_2, as depicted schematically in Figure 5. Another abundant group is $C_{10}H_{16}O_{6\text{-}12}$, which may result from RO_2 terminated by HO_2. In the dimer range, the most abundant compounds are $C_{19}H_{28}O_{8\text{-}14}$ and $C_{20}H_{30}O_{11\text{-}14}$. These compounds come from RO_2 cross reactions, as has been shown in multiple earlier studies(Ehn et al., 2014b; Jokinen et al., 2015; Mentel et al., 2015). The $C_{20}H_{30}O_n$ dimers are most likely formed from reactions of two $C_{10}H_{15}O_x$ radicals, as were many abundant monomers. As noted earlier, Cl oxidation of alkenes may occur via a Cl addition (forming an initial radical containing 16 H-atoms and one Cl atom) or via an H-abstraction reaction (forming a radical with 15 H-atoms and no Cl) (Figure 5). The abstraction pathway leads to HOM formation, or the Cl atom is lost during the subsequent reaction in the oxidation processes. With our data, we cannot rule out either of these explanations for this result. Loss of HCl from alpha-pinene products from Cl oxidation have, to our knowledge, only been reported to take place in the aerosol phase

(Ofner et al., 2013).

Figure 6 shows the variation of several close-shelled HOM products and the peroxy radical $C_{10}H_{15}O_{10}$ measured by NO_3-CI-API-TOF when we changed the lights from dark conditions to 1, 2, 4 and 7 lights switched on. Given the low Cl atom concentration, it is expected that no multi-generation oxidation by Cl can take place, and the behavior of all closed shell oxidation products should follow similar patterns. As seen in Figure 6, this was the case both for monomers and dimers. The less steep increase of the radical is also according to expectations, as the formation of RO_2 is linear with the alpha-pinene oxidation rate, but the loss rate (when dominated by RO_2 cross reactions) is proportional to $(RO_2)^2$. For closed shell species, the wall loss-driven loss rate stays constant throughout the experiment, and therefore they increase linearly with the alpha-pinene oxidation rate while the RO_2 radicals increase as the square root of the oxidation rate. For more detailed discussion on RO_2 dynamics in a steady state chamber, see Ehn et al. (2014).

In Figure7, we plotted time series of the particle number size distribution and the total number concentration, together with mass concentrations of particulate chloride and organics as we changed the number of lights. Particle formation was detected even at the lowest Cl atom concentration, as indicated by the increases in aerosol number concentration. An increase in aerosol mass concentration as detected by the AMS only took place at the two highest Cl atom concentrations, when the particles were able to grow into a size range measurable by the AMS. Particulate chloride mass concentrations also increased relatively linearly with the concentration of organics as we increased the number of lights. The Chl/Org ratio was only around 3 %, suggesting that the majority of condensed OVOC did not contain Cl atoms. However, the exact Chl quantification from organochlorides using the AMS may contain uncertainties (Wang and Ruiz, 2017), and we avoid drawing too far-reaching conclusions from this value, keeping also in mind that some fraction of the size distribution was below the lowest detectable size of our AMS. In

addition, some part of the chloride signal may also result from adsorption of HCl to particles.

3.2 Formation of HOMs at high NOx

Anthropogenic emissions have a significant influence on the formation of SOA, to a large part due to the influence of NO_x on the atmospheric oxidation chemistry (Lee et al., 2016). In general, the fate of peroxy radicals in chamber experiments can be dominated by reactions with other RO_2, HO_2 or NO, depending on the exact conditions. In our experiments without NO_x addition, RO_2 was expected to be the main terminator, as also supported by the high number of detected ROOR dimers. In the atmosphere, all of the three mentioned reaction partners may be relevant at the same time. However, with increased anthropogenic influence, the reaction of RO_2 with NO will often become dominant. Therefore, we added NO_x to the chamber as it allowed for the isolation of the formation pathways leading to HOMs in cases where NO was the main terminator for RO_2 radicals. Figure 8 depicts a HOM mass spectrum at steady state during alpha-pinene oxidation by chlorine radicals in the presence of ~10 ppb NO_x, with the maximum 7 lights turned on. As anticipated, the dimers above 440 Th were greatly reduced compared to the runs without NO_x. As more lights were turned on, both the Cl atoms and NO formation increased, as the 400 nm lights photolyze both Cl_2 and NO_2. This coupling, together with the fact that the NO_2 photolysis leads to ozone formation, which subsequently can react with alpha-pinene to form HOMs, limits our quantitative analysis of these experiments. However, we conclude that efficient HOM formation took place also under these high-NOx conditions, and thus the autoxidation occurs rapidly enough to still compete with RO_2 termination reactions. The NO_x addition also formed an abundance of organonitrate compounds like $C_{10}H_{15}NO_{8,9,10,11,12}$, as shown in Figure 8. This family of compounds may also form from H-abstraction by the chlorine radical, followed by autoxidation and finally radical termination by NO. We calculated reacted alpha-pinene from ozone and Chlorine atom as following: $[AP_{\_ozone}]/[AP_{\_Cl}]$

=[AP]*[Ozone]*2.5e10*$k_{ap+ozone}$/[AP]*[Cl]*k_{ap+Cl}, the result is around 0.2. With the results, we conclude that alpha-pinene reaction with chlorine atom is the main reaction in the system.

The concurrent formation of ozone means that also some alpha-pinene ozonolysis reaction will take place, though oxidation by Cl atoms was still the main loss for alpha-pinene also under these conditions.

Figure 9 shows variation of some nitrogen-containing HOMs and variation of alpha-pinene, ozone, NO and NO_x, as we changed the lights from dark conditions to 1, 2, 4 or 7 lights switched on. The concentrations of alpha-pinene and NO_2 decreased because of the consumption by chlorine radicals and photolysis of NO_2 into NO. Importantly, we did not observe any SOA when we had NO in the chamber. NO may have suppressed the particle formation by suppressing the dimer formation, as these have been shown to be important for initial particle formation (Tröstl et al., 2016).

3.3 Estimated HOMs production yields

Quantifying the molar yields of HOMs is essential to know their potential importance from a specific system. We attempt to estimate the molar yield in the case of Cl oxidation of alpha-pinene in the absence of NO_x. The initial $C_{10}H_{16}$ concentration is around 13.3 ppb without any UV lights switched on in the chamber. As we changed the lights, alpha-pinene and HOM concentrations varied as we showed in Figure 3. In addition, we calculated the concentration of Cl radicals as introduced in the Methods section. With this information, we can calculate the formation rate of HOM, which in steady state equals the HOM loss rate [HOM]*k_{loss}. We can also calculate the oxidation rate of alpha-pinene as [alpha-pinene]*[Cl]*k_{AP+Cl}. The ratio of these two numbers corresponds to the HOM molar yield. We selected the same runs as in Fig. 3, used also for calculating the chlorine radical concentration, and calculated the ratio as a linear fit to these four conditions (Figure 10). We get a slope of 0.018, meaning a HOM yield of 1.8%. Considering the uncertainty in estimating absolute HOM concentrations, we

conservatively estimate that the molar HOM yield from alpha-pinene + Cl is within the range of 0.8-4 %. These values are similar to HOM yields reported for alpha-pinene oxidation by ozone and OH (Berndt et al., 2016; Ehn et al., 2014).

4.Conclusion

We have systematically explored the reactions of alpha-pinene with chlorine atoms in a simulation smog chamber under atmospherically relevant conditions. We measured substantial amounts of highly oxidized organic molecules (HOM) with a NO_3-CI-API-TOF. With increasing UV lights, and consequently higher chlorine radical concentrations, the concentrations of both HOM and secondary organic aerosol increased. With addition of NOx, HOM monomer formation was still efficient, but the particle formation decreased greatly. We estimated HOM molar yields of around 1.8 % (0.8-4 %) from the reaction of alpha-pinene with Cl atoms. Our study thus indicates that in regions where chlorine atom oxidation is of importance, its possible reactions with monoterpenes can be an important source of HOM, and consequently, SOA.

Acknowledgement

This work is supported by European Research Council (Grant 638703-COALA) project and Academy of Finland, via the Center of Excellence in Atmospheric Sciences and project numbers 317380 and 320094. We acknowledge the Toftools team for providing the software.

Competing financial interests

The authors declare no competing financial interests.

Author contributions

Y. H. W, H. B. X and M. E had the original idea of the study. Y. H. W, M. R and H. B. X conducted the chamber experiments. Y. H. W, M. R, H. B. X, L.H and M. E interpreted the data. Y.H.W plotted the figures, wrote the manuscript with comments and suggestions from all co-authors.

Reference

Berndt, T., Richters, S., Jokinen, T., Hyttinen, N., Kurtén, T., Otkjaer, R. V,

Kjaergaard, H. G., Stratmann, F., Herrmann, H., Sipilä, M., Kulmala, M. and Ehn, M.: ARTICLE Hydroxyl radical-induced formation of highly oxidized organic compounds, , doi:10.1038/ncomms13677, 2016a.

Berndt, T., Richters, S., Jokinen, T., Hyttinen, N., Kurtén, T., Otkjær, R. V, Kjaergaard, H. G., Stratmann, F., Herrmann, H., Sipilä, M., Kulmala, M. and Ehn, M.: Hydroxyl radical-induced formation of highly oxidized organic compounds, Nature Communications, 7, 13677 [online] Available from: https://doi.org/10.1038/ncomms13677, 2016b.

Bianchi, F., Kurtén, T., Riva, M., Mohr, C., Rissanen, M. P., Roldin, P., Berndt, T., Crounse, J. D., Wennberg, P. O., Mentel, T. F., Wildt, J., Junninen, H., Jokinen, T., Kulmala, M., Worsnop, D. R., Thornton, J. A., Donahue, N., Kjaergaard, H. G. and Ehn, M.: Highly Oxygenated Organic Molecules (HOM) from Gas-Phase Autoxidation Involving Peroxy Radicals: A Key Contributor to Atmospheric Aerosol, Chemical Reviews, 119(6), 3472–3509, doi:10.1021/acs.chemrev.8b00395, 2019.

Cai, X. and Griffin, R. J.: Secondary aerosol formation from the oxidation of biogenic hydrocarbons by chlorine atoms, Journal of Geophysical Research Atmospheres, 111(14), 1–14, doi:10.1029/2005JD006857, 2006.

Crounse, J. D., Nielsen, L. B., Jørgensen, S., Kjaergaard, H. G. and Wennberg, P. O.: Autoxidation of organic compounds in the atmosphere, Journal of Physical Chemistry Letters, 4(20), 3513–3520, doi:10.1021/jz4019207, 2013.

Decarlo, P. F., Kimmel, J. R., Trimborn, A., Northway, M. J., Jayne, J. T., Aiken, A. C., Gonin, M., Fuhrer, K., Horvath, T., Docherty, K. S., Worsnop, D. R. and Jimenez, J. L.: Field-Deployable, High-Resolution, Time-of-Flight Aerosol Mass Spectrometer, Analytical Chemistry, 78, 8281–8289, doi:10.1021/ac061249n, 2006.

Ehn, M., Thornton, J. A., Kleist, E., Sipilä, M., Junninen, H., Pullinen, I., Springer, M., Rubach, F., Tillmann, R., Lee, B., Lopez-Hilfiker, F., Andres, S., Acir, I.-H., Rissanen, M., Jokinen, T., Schobesberger, S., Kangasluoma, J., Kontkanen, J., Nieminen, T., Kurtén, T., Nielsen, L. B., Jørgensen, S., Kjaergaard, H. G., Canagaratna, M., Maso, M. D., Berndt, T., Petäjä, T., Wahner, A., Kerminen, V.-M.,

Kulmala, M., Worsnop, D. R., Wildt, J. and Mentel, T. F.: A large source of low-volatility secondary organic aerosol, Nature, 506(7489), 476–479, doi:10.1038/nature13032, 2014a.

Ehn, M., Thornton, J. A., Kleist, E., Sipilä, M., Junninen, H., Pullinen, I., Springer, M., Rubach, F., Tillmann, R., Lee, B., Lopez-Hilfiker, F., Andres, S., Acir, I.-H., Rissanen, M., Jokinen, T., Schobesberger, S., Kangasluoma, J., Kontkanen, J., Nieminen, T., Kurtén, T., Nielsen, L. B., Jørgensen, S., Kjaergaard, H. G., Canagaratna, M., Dal Maso, M., Berndt, T., Petäjä, T., Wahner, A., Kerminen, V.-M., Kulmala, M., Worsnop, D. R., Wildt, J. and Mentel, T. F.: A large source of low-volatility secondary organic aerosol, Nature, 506, doi:10.1038/nature13032, 2014b.

Ehn, M., Berndt, T., Wildt, U. and Mentel, T.: Highly Oxygenated Molecules from Atmospheric Autoxidation of Hydrocarbons: A Prominent Challenge for Chemical Kinetics Studies, International journal of chemical knineticsinetics, 821–831, doi:10.1002/kin.21130, 2017.

Finlayson-Pitts, B. J., Keoshian, C. J., Buehler, B. and Ezell, A. A.: Kinetics of Reaction of Chlorine Atoms with Some, International Journal of Chemical Kinetics, 31, 491–499, 1999.

Guenther, A., Hewitt, C. N., Erickson, D., Fall, R., Geron, C., Graedel, T., Harley, P., Klinger, L., Lerdau, M., Mckay, W. A., Pierce, T., Scholes, B., Steinbrecher, R., Tallamraju, R., Taylor, J. and Zimmerman, P.: A global model of natural volatile organic compound emissions, Journal of Geophysical Research: Atmospheres, 100(D5), 8873–8892, doi:10.1029/94JD02950, 1995.

Jokinen, T., Sipilä, M., Junninen, H., Ehn, M., Lönn, G., Hakala, J., Petäjä, T., Mauldin Iii, R. L., Kulmala, M. and Worsnop, D. R.: Atmospheric sulphuric acid and neutral cluster measurements using CI-APi-TOF, Atmos. Chem. Phys. Atmospheric Chemistry and Physics, 12, 4117–4125, doi:10.5194/acp-12-4117-2012, 2012.

Jokinen, T., Sipilä, M., Richters, S., Kerminen, V., Paasonen, P., Stratmann, F., Worsnop, D., Kulmala, M., Ehn, M., Herrmann, H. and Berndt, T.: Rapid Autoxidation Forms Highly Oxidized RO 2 Radicals in the Atmosphere **

Angewandte, , 1–6, doi:10.1002/anie.201408566, 2014a.
Jokinen, T., Sipilä, M., Richters, S., Kerminen, V. M., Paasonen, P., Stratmann, F., Worsnop, D., Kulmala, M., Ehn, M., Herrmann, H. and Berndt, T.: Rapid autoxidation forms highly oxidized RO2 radicals in the atmosphere, Angewandte Chemie - International Edition, 53(52), 14596–14600, doi:10.1002/anie.201408566, 2014b.
Jokinen, T., Berndt, T., Makkonen, R., Kerminen, V.-M., Junninen, H., Paasonen, P., Stratmann, F., Herrmann, H., Guenther, A. B., Worsnop, D. R., Kulmala, M., Ehn, M. and Sipilä, M.: Production of extremely low volatile organic compounds from biogenic emissions: Measured yields and atmospheric implications, Proceedings of the National Academy of Sciences, 112(23), 7123–7128, doi:10.1073/pnas.1423977112, 2015.
Jonsson, Å. M., Hallquist, M. and Ljungström, E.: Impact of humidity on the ozone initiated oxidation of limonene, Δ3-carene, and α-pinene, Environmental Science and Technology, 40(1), 188–194, doi:10.1021/es051163w, 2006.
Jonsson, Å. M., Hallquist, M. and Ljungström, E.: Influence of OH scavenger on the water effect on secondary organic aerosol formation from ozonolysis of limonene, Δ3-carene, and α-pinene, Environmental Science and Technology, 42(16), 5938–5944, doi:10.1021/es702508y, 2008.
Kulmala, M., Kontkanen, J., Junninen, H., Lehtipalo, K., Manninen, H. E., Nieminen, T., Petäjä, T., Sipilä, M., Schobesberger, S., Rantala, P., Franchin, A., Jokinen, T., Järvinen, E., Äijälä, M., Kangasluoma, J., Hakala, J., Aalto, P. P., Paasonen, P., Mikkilä, J., Vanhanen, J., Aalto, J., Hakola, H., Makkonen, U., Ruuskanen, T., Mauldin, R. L., Duplissy, J., Vehkamäki, H., Bäck, J., Kortelainen, A., Riipinen, I., Kurtén, T., Johnston, M. V., Smith, J. N., Ehn, M., Mentel, T. F., Lehtinen, K. E. J., Laaksonen, A., Kerminen, V. M. and Worsnop, D. R.: Direct observations of atmospheric aerosol nucleation, Science, 339(6122), 943–946, doi:10.1126/science.1227385, 2013.
Lee, B. H., Mohr, C., Lopez-Hilfiker, F. D., Lutz, A., Hallquist, M., Lee, L., Romer,

P., Cohen, R. C., Iyer, S., Kurtén, T., Hu, W., Day, D. A., Campuzano-Jost, P., Jimenez, J. L., Xu, L., Ng, N. L., Guo, H., Weber, R. J., Wild, R. J., Brown, S. S., Koss, A., de Gouw, J., Olson, K., Goldstein, A. H., Seco, R., Kim, S., McAvey, K., Shepson, P. B., Starn, T., Baumann, K., Edgerton, E. S., Liu, J., Shilling, J. E., Miller, D. O., Brune, W., Schobesberger, S., D'Ambro, E. L. and Thornton, J. A.: Highly functionalized organic nitrates in the southeast United States: Contribution to secondary organic aerosol and reactive nitrogen budgets, Proceedings of the National Academy of Sciences, 113(6), 1516–1521, doi:10.1073/pnas.1508108113, 2016.

Li, X., Chee, S., Hao, J., Abbatt, J. P. D., Jiang, J. and Smith, J. N.: Relative humidity effect on the formation of highly oxidized molecules and new particles during monoterpene oxidation, Atmospheric Chemistry and Physics, 19(3), 1555–1570, doi:10.5194/acp-19-1555-2019, 2019.

Liu, X., Qu, H., Huey, L. G., Wang, Y., Sjostedt, S., Zeng, L., Lu, K., Wu, Y., Hu, M., Shao, M., Zhu, T. and Zhang, Y.: High Levels of Daytime Molecular Chlorine and Nitryl Chloride at a Rural Site on the North China Plain, Environ Sci Technol, 51, 9588–9595, doi:10.1021/acs.est.7b03039, 2017.

Mentel, T. F., Springer, M., Ehn, M., Kleist, E., Pullinen, I., Kurtén, T., Rissanen, M., Wahner, A. and Wildt, J.: Formation of highly oxidized multifunctional compounds: autoxidation of peroxy radicals formed in the ozonolysis of alkenes – deduced from structure–product relationships, Atmos. Chem. Phys, 15, 6745–6765, doi:10.5194/acp-15-6745-2015, 2015.

Ofner, J., Kamilli, K. A., Held, A., Lendl, B. and Zetzsch, C.: Halogen-induced organic aerosol (XOA): a study on ultra-fine particle formation and time-resolved chemical characterization, Faraday Discussions, 165, 135, doi:10.1039/c3fd00093a, 2013.

Peräkylä, O., Riva, M., Heikkinen, L., Quéléver, L., Roldin, P. and Ehn, M.: Experimental investigation into the volatilities of highly oxygenated organic molecules (HOM), , (July), 1–28, 2019.

Praske, E., Otkjær, R. V, Crounse, J. D., Hethcox, J. C., Stoltz, B. M., Kjaergaard, H.

505 G. and Wennberg, P. O.: Atmospheric autoxidation is increasingly important in urban
506 and suburban North America, Proceedings of the National Academy of Sciences,
507 115(1), 64 LP – 69, doi:10.1073/pnas.1715540115, 2018.
508 Reyes-Villegas, E., Priestley, M., Ting, Y.-C., Haslett, S., Bannan, T., Le Breton, M.,
509 Williams, P. I., Bacak, A., Flynn, M. J., Coe, H., Percival, C. and Allan, J. D.:
510 Simultaneous aerosol mass spectrometry and chemical ionisation mass spectrometry
511 measurements during a biomass burning event in the UK: insights into nitrate
512 chemistry, Atmos. Chem. Phys, 185194, 4093–4111, doi:10.5194/acp-18-4093-2018,
513 2018.
514 Riccobono, F., Schobesberger, S., Scott, C. E., Dommen, J., Ortega, I. K., Rondo, L.,
515 Almeida, J., Amorim, A., Bianchi, F., Breitenlechner, M., David, A., Downard, A.,
516 Dunne, E. M., Duplissy, J., Ehrhart, S., Flagan, R. C., Franchin, A., Hansel, A.,
517 Junninen, H., Kajos, M., Keskinen, H., Kupc, A., Kürten, A., Kvashin, A. N.,
518 Laaksonen, A., Lehtipalo, K., Makhmutov, V., Mathot, S., Nieminen, T., Onnela, A.,
519 Petäjä, T., Praplan, A. P., Santos, F. D., Schallhart, S., Seinfeld, J. H., Sipilä, M.,
520 Spracklen, D. V, Stozhkov, Y., Stratmann, F., Tomé, A., Tsagkogeorgas, G.,
521 Vaattovaara, P., Viisanen, Y., Vrtala, A., Wagner, P. E., Weingartner, E., Wex, H.,
522 Wimmer, D., Carslaw, K. S., Curtius, J., Donahue, N. M., Kirkby, J., Kulmala, M.,
523 Worsnop, D. R. and Baltensperger, U.: Oxidation Products of Biogenic Emissions
524 Contribute to Nucleation of Atmospheric Particles, Science, 344(717),
525 doi:10.1126/science.1243527, 2014.
526 Rissanen, M. P., Kurtén, T., Sipilä, M., Thornton, J. A., Kangasluoma, J., Sarnela, N.,
527 Junninen, H., Jørgensen, S., Schallhart, S., Kajos, M. K., Taipale, R., Springer, M.,
528 Mentel, T. F., Ruuskanen, T., Petäjä, T., Worsnop, D. R., Kjaergaard, H. G. and Ehn,
529 M.: The formation of highly oxidized multifunctional products in the ozonolysis of
530 cyclohexene, Journal of the American Chemical Society, 136(44), 15596–15606,
531 doi:10.1021/ja507146s, 2014.
532 Riva, M., Healy, R. M., Flaud, P. M., Perraudin, E., Wenger, J. C. and Villenave, E.:
533 Gas- and Particle-Phase Products from the Chlorine-Initiated Oxidation of Polycyclic

Aromatic Hydrocarbons, Journal of Physical Chemistry A, 119(45), 11170–11181, doi:10.1021/acs.jpca.5b04610, 2015.

Riva, M., Heikkinen, L., Bell, D. M., Peräkylä, O., Zelenyuk, A. and Ehn, M.: Chemical transformations in monoterpene-derived organic aerosol enhanced by inorganic composition, npj Climate and Atmospheric Science, (July 2018), 1–9, doi:10.1038/s41612-018-0058-0, 2019a.

Riva, M., Rantala, P., Krechmer, E. J., Peräkylä, O., Zhang, Y., Heikkinen, L., Garmash, O., Yan, C., Kulmala, M., Worsnop, D. and Ehn, M.: Evaluating the performance of five different chemical ionization techniques for detecting gaseous oxygenated organic species, Atmospheric Measurement Techniques, 12(4), 2403–2421, doi:10.5194/amt-12-2403-2019, 2019b.

Schallhart, S., Rantala, P., Kajos, M. K., Aalto, J., Mammarella, I., Ruuskanen, T. M. and Kulmala, M.: Temporal variation of VOC fluxes measured with PTR-TOF above a boreal forest, Atmospheric Chemistry and Physics, 18(2), 815–832, doi:10.5194/acp-18-815-2018, 2018.

Tham, Y. J., Wang, Z., Li, Q., Yun, H., Wang, W., Wang, X., Xue, L., Lu, K., Ma, N., Bohn, B., Li, X., Kecorius, S., Größ, J., Shao, M., Wiedensohler, A., Zhang, Y. and Wang, T.: Significant concentrations of nitryl chloride sustained in the morning: investigations of the causes and impacts on ozone production in a polluted region of northern China, Atmos. Chem. Phys, 16, 14959–14977, doi:10.5194/acp-16-14959-2016, 2016.

Thornton, J. A., Kercher, J. P., Riedel, T. P., Wagner, N. L., Cozic, J., Holloway, J. S., Dubé, W. P., Wolfe, G. M., Quinn, P. K., Middlebrook, A. M., Alexander, B. and Brown, S. S.: A large atomic chlorine source inferred from mid-continental reactive nitrogen chemistry, Nature, 464(7286), 271–274, doi:10.1038/nature08905, 2010a.

Thornton, J. A., Kercher, J. P., Riedel, T. P., Wagner, N. L., Cozic, J., Holloway, J. S., Dubé, W. P., Wolfe, G. M., Quinn, P. K., Middlebrook, A. M., Alexander, B. and Brown, S. S.: A large atomic chlorine source inferred from mid-continental reactive nitrogen chemistry, Nature, 464(7286), 271–274, doi:10.1038/nature08905, 2010b.

563 Tröstl, J., Chuang, W. K., Gordon, H., Heinritzi, M., Yan, C., Molteni, U., Ahlm, L.,
564 Frege, C., Bianchi, F., Wagner, R., Simon, M., Lehtipalo, K., Williamson, C., Craven,
565 J. S., Duplissy, J., Adamov, A., Almeida, J., Bernhammer, A.-K., Breitenlechner, M.,
566 Brilke, S., Dias, A., Ehrhart, S., Flagan, R. C., Franchin, A., Fuchs, C., Guida, R.,
567 Gysel, M., Hansel, A., Hoyle, C. R., Jokinen, T., Junninen, H., Kangasluoma, J.,
568 Keskinen, H., Kim, J., Krapf, M., Kürten, A., Laaksonen, A., Lawler, M., Leiminger,
569 M., Mathot, S., Möhler, O., Nieminen, T., Onnela, A., Petäjä, T., Piel, F. M.,
570 Miettinen, P., Rissanen, M. P., Rondo, L., Sarnela, N., Schobesberger, S., Sengupta,
571 K., Sipilä, M., Smith, J. N., Steiner, G., Tomè, A., Virtanen, A., Wagner, A. C.,
572 Weingartner, E., Wimmer, D., Winkler, P. M., Ye, P., Carslaw, K. S., Curtius, J.,
573 Dommen, J., Kirkby, J., Kulmala, M., Riipinen, I., Worsnop, D. R., Donahue, N. M.
574 and Baltensperger, U.: The role of low-volatility organic compounds in initial particle
575 growth in the atmosphere, Nature, 533(7604), 527–531, doi:10.1038/nature18271,
576 2016.
577 Wang, D. S. and Ruiz, L. H.: Secondary organic aerosol from chlorine-initiated
578 oxidation of isoprene, Atmospheric Chemistry and Physics, 17(22), 13491–13508,
579 doi:10.5194/acp-17-13491-2017, 2017.
580 Wang, Z., Wang, W., Tham, Y. J., Li, Q., Wang, H., Wen, L., Wang, X. and Wang,
581 T.: Fast heterogeneous N 2 O 5 uptake and ClNO 2 production in power plant and
582 industrial plumes observed in the nocturnal residual layer over the North China Plain,
583 Atmos. Chem. Phys, 175194, 12361–12378, doi:10.5194/acp-17-12361-2017, 2017.
584 Zhang, H., Yee, L. D., Lee, B. H., Curtis, M. P., Worton, D. R., Isaacman-VanWertz,
585 G., Offenberg, J. H., Lewandowski, M., Kleindienst, T. E., Beaver, M. R., Holder, A.
586 L., Lonneman, W. A., Docherty, K. S., Jaoui, M., Pye, H. O. T., Hu, W., Day, D. A.,
587 Campuzano-Jost, P., Jimenez, J. L., Guo, H., Weber, R. J., de Gouw, J., Koss, A. R.,
588 Edgerton, E. S., Brune, W., Mohr, C., Lopez-Hilfiker, F. D., Lutz, A., Kreisberg, N.
589 M., Spielman, S. R., Hering, S. V., Wilson, K. R., Thornton, J. A. and Goldstein, A.
590 H.: Monoterpenes are the largest source of summertime organic aerosol in the
591 southeastern United States, Proceedings of the National Academy of Sciences,

201717513, doi:10.1073/pnas.1717513115, 2018.

Figure and table captions

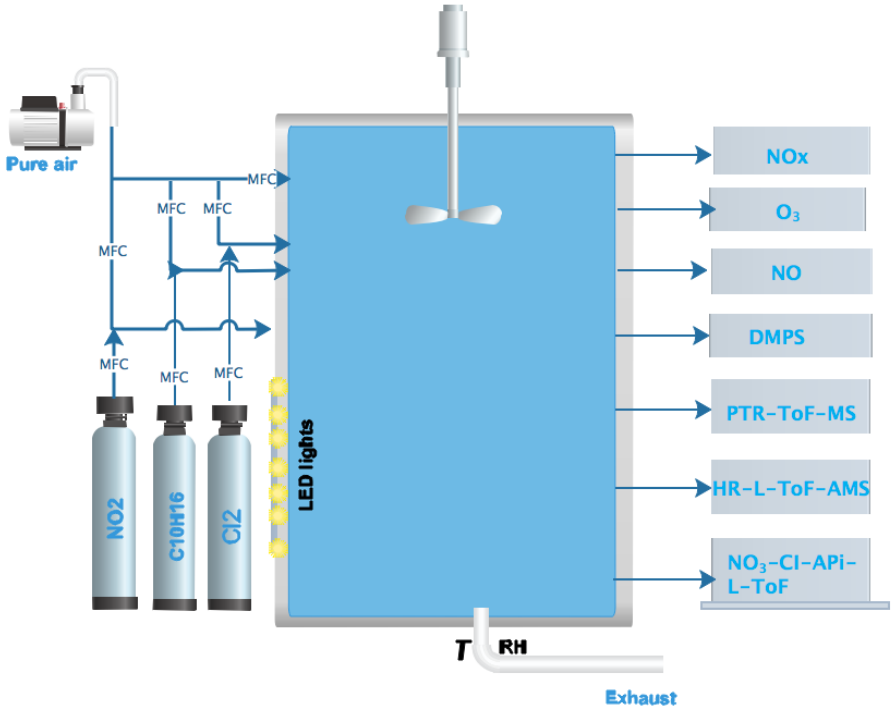

Figure 1 A schematic of the chamber setup and instruments used in the experiment.

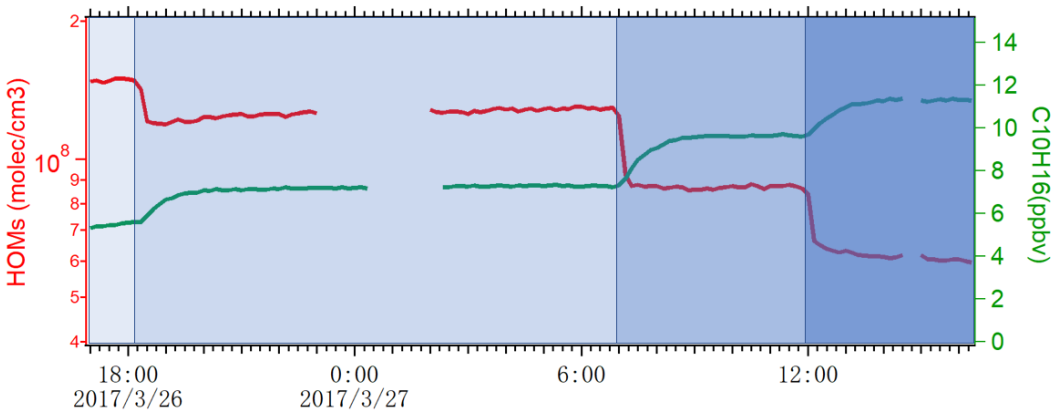

Figure 2. The variation of total HOM concentration and alpha-pinene during four experiments where the 400 nm lights were decreased stepwise from 7 lights to 4, 2 and 1 light, respectively.

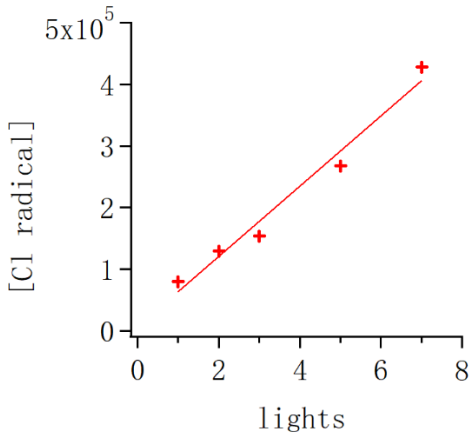

644

645 Figure 3. The variation of chlorine radical concentration as a function of lights. The

646 input alpha-pinene concentration was kept constant throughout the experiments.

647

648

649

650

651

652

653

654

655

656

657

658

659

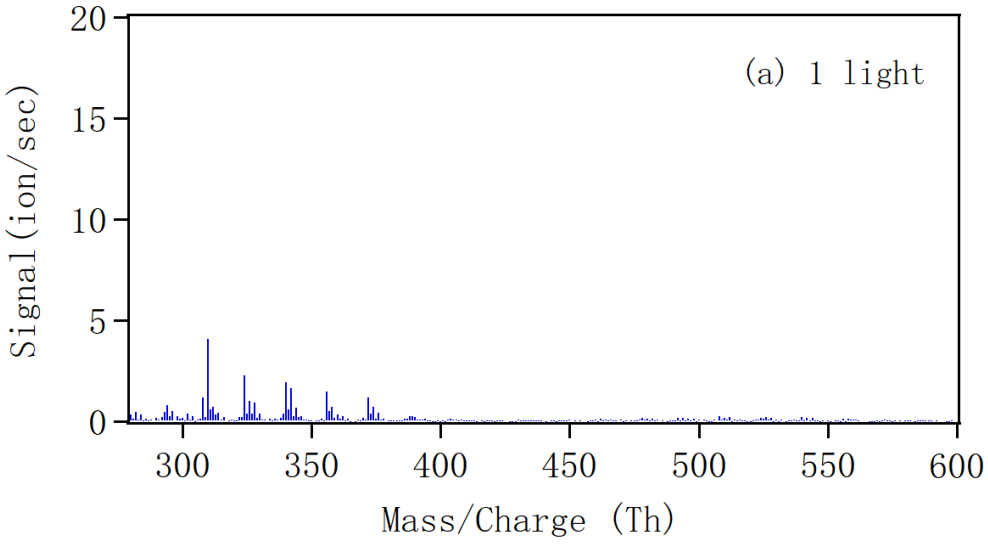
(a) 1 light
Signal (ion/sec)
Mass/Charge (Th)
0
5
10
15
20
300
350
400
450
500
550
600

660

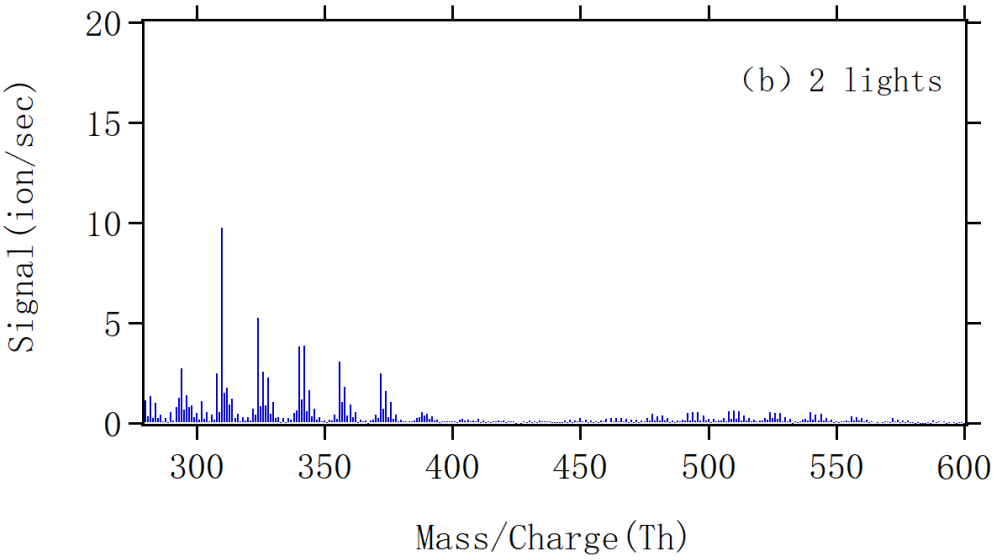
(b) 2 lights
Signal (ion/sec)
Mass/Charge (Th)
0
5
10
15
20
300
350
400
450
500
550
600

661

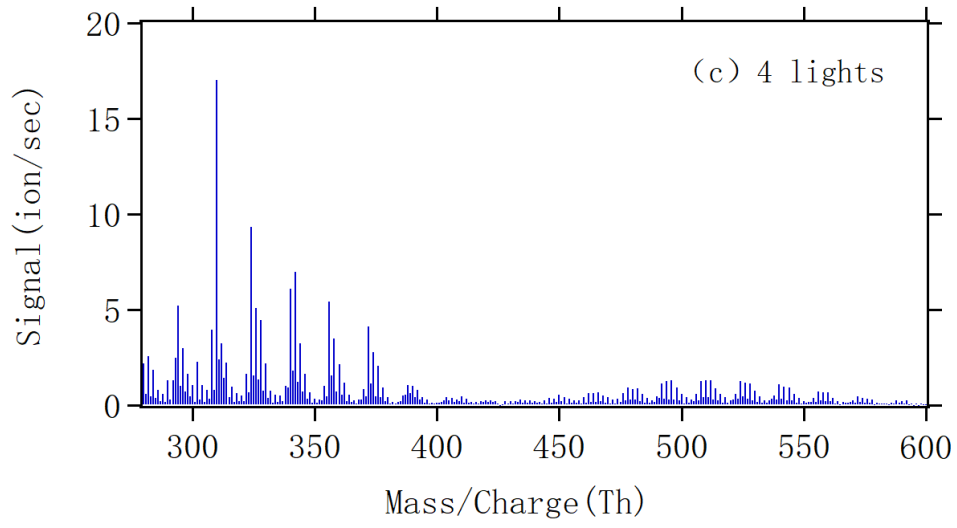
(c) 4 lights
Signal (ion/sec)
Mass/Charge (Th)
0
5
10
15
20
300
350
400
450
500
550
600

662

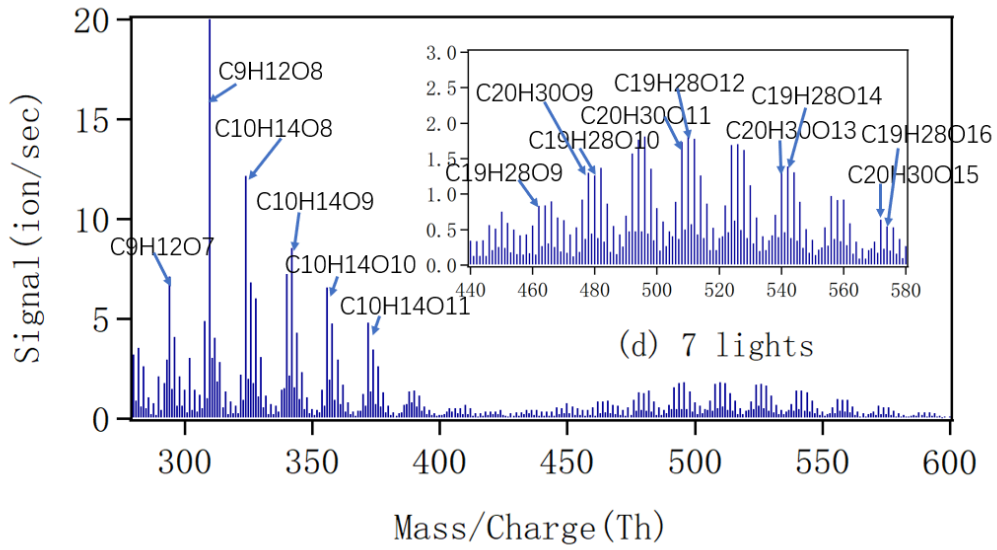

Figure 4. The mass spectra obtained by NO_3-CI-API-TOF during steady state with 1(a), 2(b), 4(c) and 7(d) lights. All peaks are detected as clusters with NO_3-. The spectra are plotted as unit mass resolution, with background signals removed, but the peak identifications (labeled in panel d) are based on high resolution analyses. The spectra correspond to the same four steady state conditions depicted in Fig. 2.

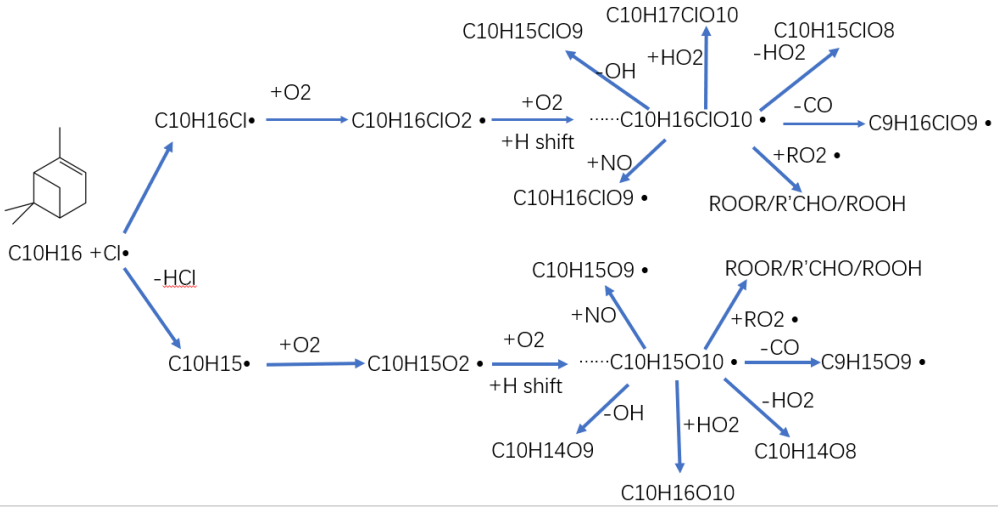

Figure 5. Proposed chemical pathways for chlorine radical oxidation of alpha-pinene, and subsequent autoxidation and HOM formation. The upper path shows the chlorine radical addition pathway, while the lower chain shows hydrogen atom abstraction pathway. In both cases, initially a C-centered radical forms ($C_{10}H_{16}Cl$ or $C_{10}H_{15}$) to which O_2 adds to form an initial peroxy radical. This peroxy radical may then undergo multi-step autoxidation to reach the example molecules $C_{10}H_{16}ClO_{10}$ or $C_{10}H_{15}O_{10}$ before termination.

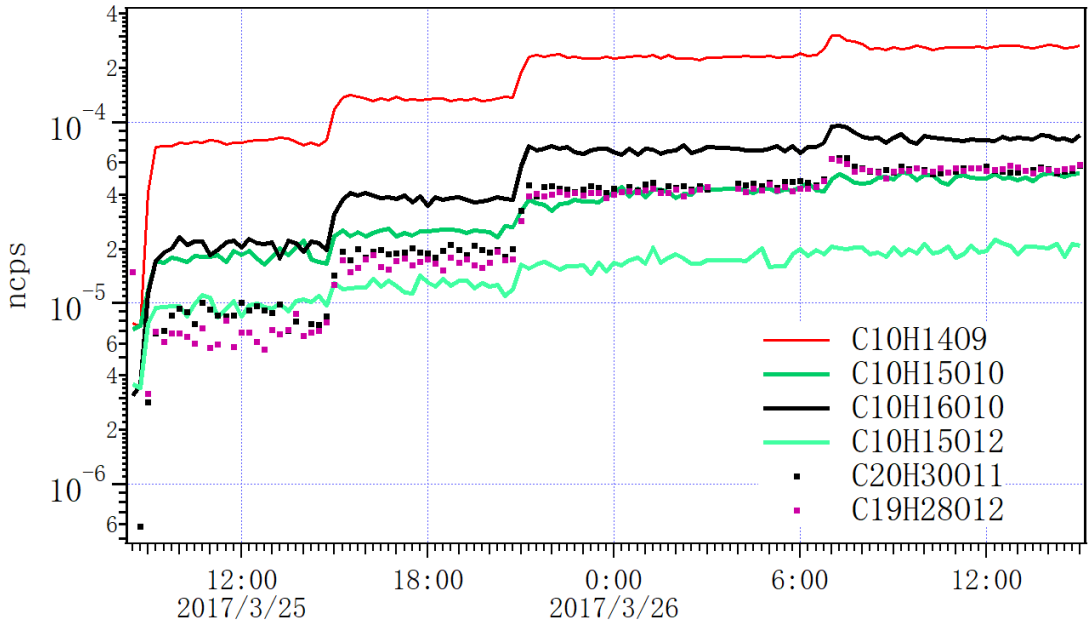

689

690

691

692

693 Figure 6. Time series of selected closed-shell HOM monomers, dimers and an RO_2

694 radical ($C_{10}H_{15}O_{10}$) detected by NO_3-CI-APi-TOF as the lights increased from 0 to 1,

695 2, 4 and 7.

696

697

698

699

700

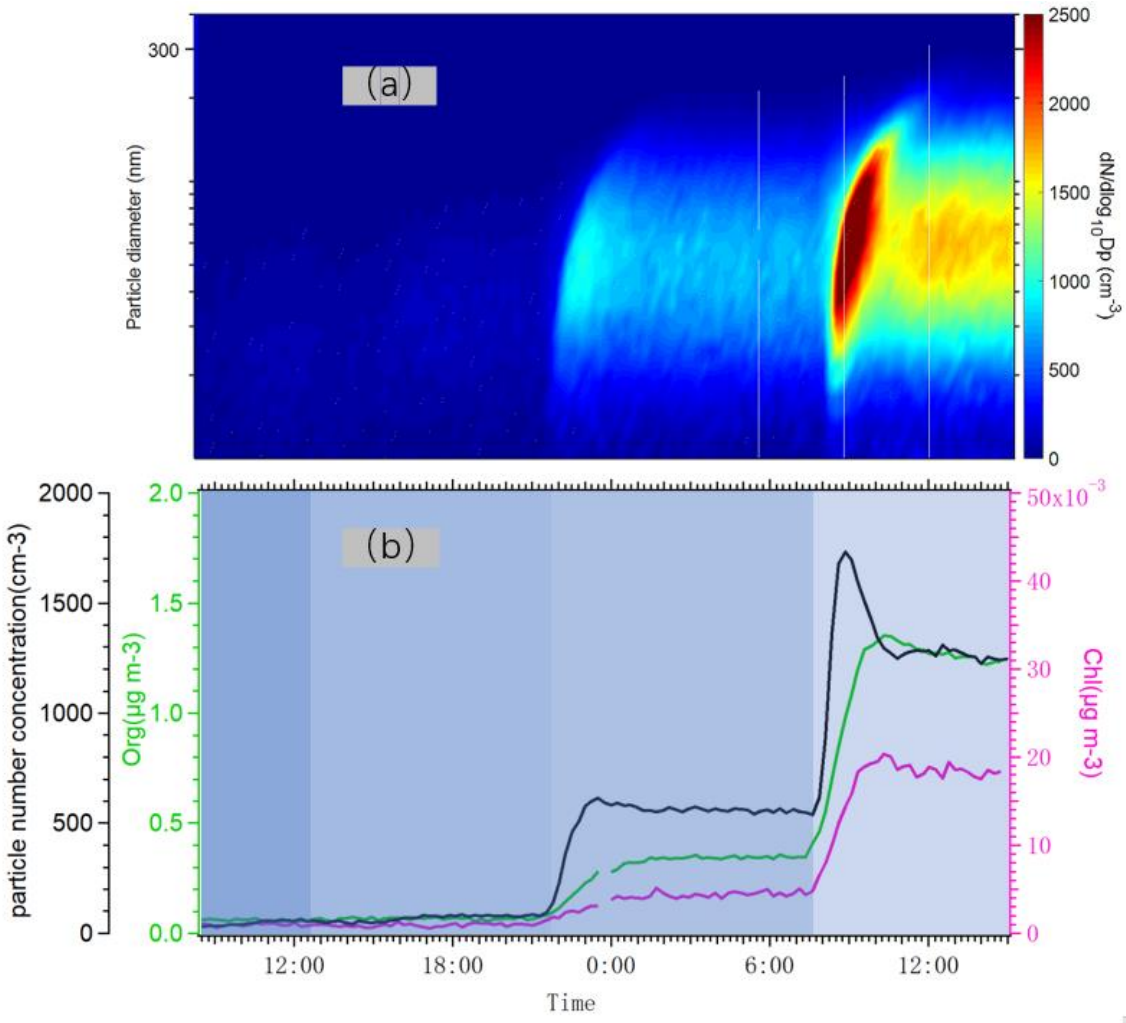

Figure 7. (a) Particle number size distribution measured by DMPS from 10 nm to 400nm when the lights varied from 1 to 2, 4 and 7. (b) Time series of total number concentration (black) measured by DMPS, organic aerosol concentration (green) and particulate chloride concentration (pink)measured by AMS.

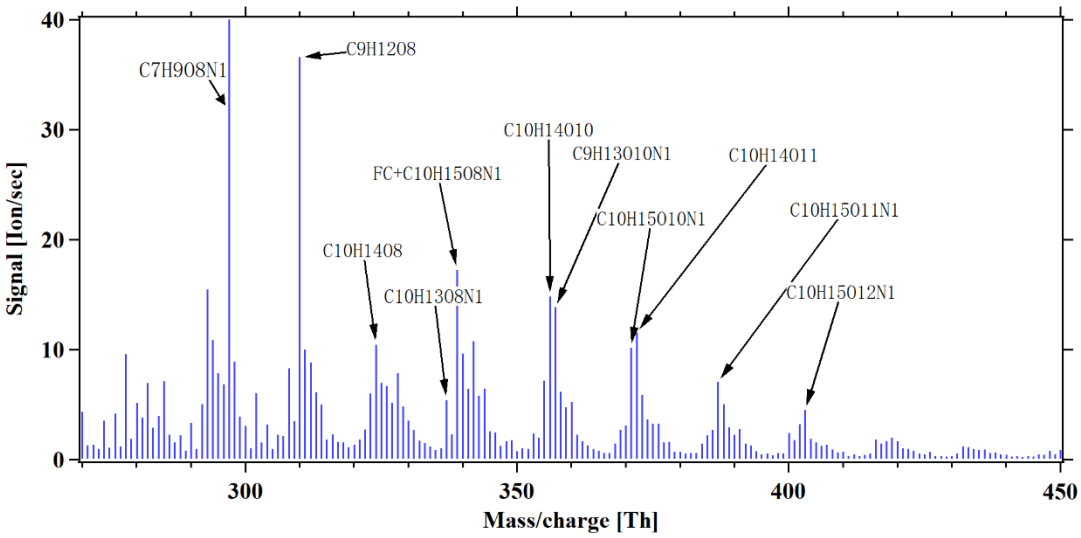

Figure 8. HOM mass spectrum during steady state alpha-pinene oxidation in the presence of 10 ppb NOx, with 7 lights switched on. In addition to molecules detected also in the experiments without NOx, several abundant organic nitrate peaks are formed. Note that a fluorinated compounds (FC) overlaps with the organ nitrate $C_{10}H_{15}O_8N$ at 339Th. All peaks are detected as clusters with NO_3-.

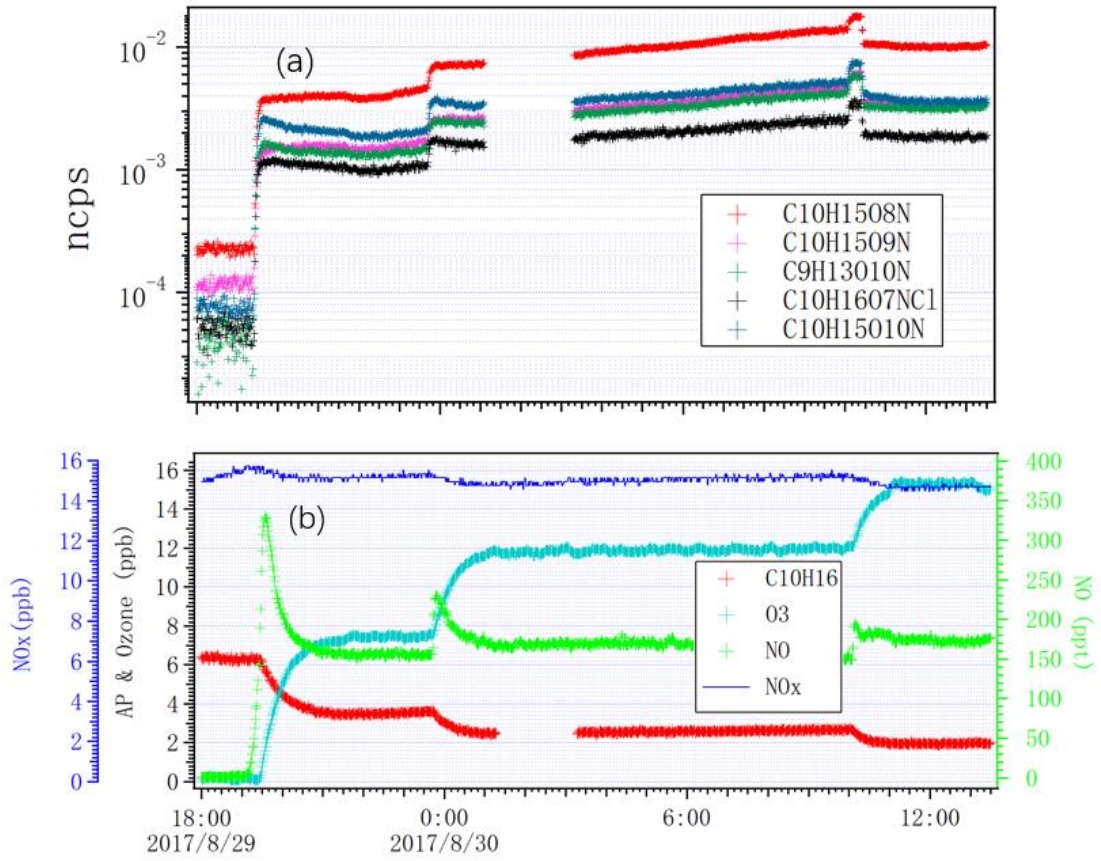

Figure 9. Time series of (a) selected HOMs measured by NO_3-CI-L-API-TOF and (b) NO_x, a-pinene, ozone and NO, as the lights switched on from zero to 2, 4, and 7.

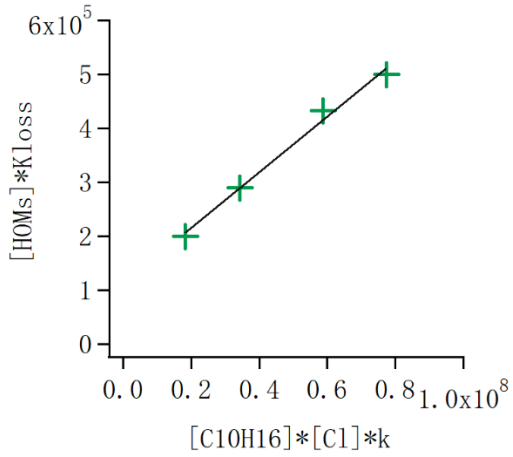

743

744

745 Figure 10. HOM loss rate ([HOM]*Kloss) as a function of the alpha-pinene
746 oxidation rate. In steady state the loss rate equals the formation rate, and thus
747 the slope of the points gives the molar yield of HOM from the alpha-pinene +
748 Cl reaction. The data corresponds to the conditions with 1, 2, 4 and 7 lights
749 switched on in the chamber, respectively. The slope indicates an average molar
750 yield of HOMs of 1.8%.

751

752

753